ELSEVIER
Tectonophysics 302 (1999) 57–69

2-D geoelectrical model for the Parnaíba Basin conductivity anomaly of northeast Brazil and tectonic implications

B.R. Arora [a,1], A.L. Padilha [a], Í. Vitorello [a,*], N.B. Trivedi [a], S.L. Fontes [b], A. Rigoti [c], F.H. Chamalaun [d]

[a] *Instituto Nacional de Pesquisas Espaciais, INPE, DGE, C.P. 515, 12201-970 São José dos Campos, S.P., Brazil*
[b] *Departamento de Geofísica, CNPq-Observatório Nacional, C.P. 23002, 20921-400 Rio de Janeiro, Brazil*
[c] *Departamento de Geologia, Universidade Federal do Paraná, C.P. 19011, 81531-990 Curitiba, Brazil*
[d] *School of Earth Sciences, Flinders University of South Australia, G.P.O. Box 2100, Adelaide, S.A. 5001, Australia*

Received 16 September 1997; accepted 30 October 1998

Abstract

A magnetometer array study in the north-northeast of Brazil has revealed a roughly NE–SW-trending conductive structure in the southeastern part of the intracratonic Parnaíba Basin. The magnetovariational response functions of this structure are numerically modelled to constrain its geometry to facilitate its geological and tectonic interpretation. The 2-D numerical model that incorporates the ocean effect and can account for the spatial and period dependence of the observed response locates the source regions of enhanced conductivity in a graben structure in the basement as well as in a block confined to the central part of the basin with an embedded resistive body. The anomalous electrical character of the sediments in the central part of the basin is consistent with the magnetotelluric data, the graben structure in the basement is corroborated by the aeromagnetic data. The formation of the graben structure is considered to be a manifestation of the extensional tectonics associated either with the Brasiliano orogeny or with the Jurassic–Cretaceous magmatic events. The diabase dikes intruded in the basin in association with the Jurassic–Cretaceous magmatic activity are shown to be accountable for the mapped resistive body entrapped in the conducting Paleozoic sediments. The thermal effects associated with magmatic activities are invoked to produce enhanced conductivity by the generation of carbon through the pyrolysis of hydrocarbon-saturated sediments.

Keywords: electromagnetic induction; magnetovariational fields; conductivity anomalies; geoelectrical modelling; intracratonic basin; magmatic activity

1. Introduction

An earlier paper (Arora et al., 1998a) reported the presence of a variety of conductive structures in the north-northeast of Brazil. The existence of the conductive structures was deduced from the analysis and interpretation of magnetovariational (MV) fields recorded by an array of 29 magnetometers operated in and around the region of the intracratonic Parnaíba Basin. Fig. 1 shows the distribution of the magnetometer sites against the geological background of the Parnaíba Basin and contiguous tectonic features.

* Corresponding author: E-mail: icaro@dge.inpe.br
[1] Present address: Indian Institute of Geomagnetism Colaba, Mumbai 400005, India.

0040-1951/99/$ – see front matter
PII: S0040-1951(98)00272-8

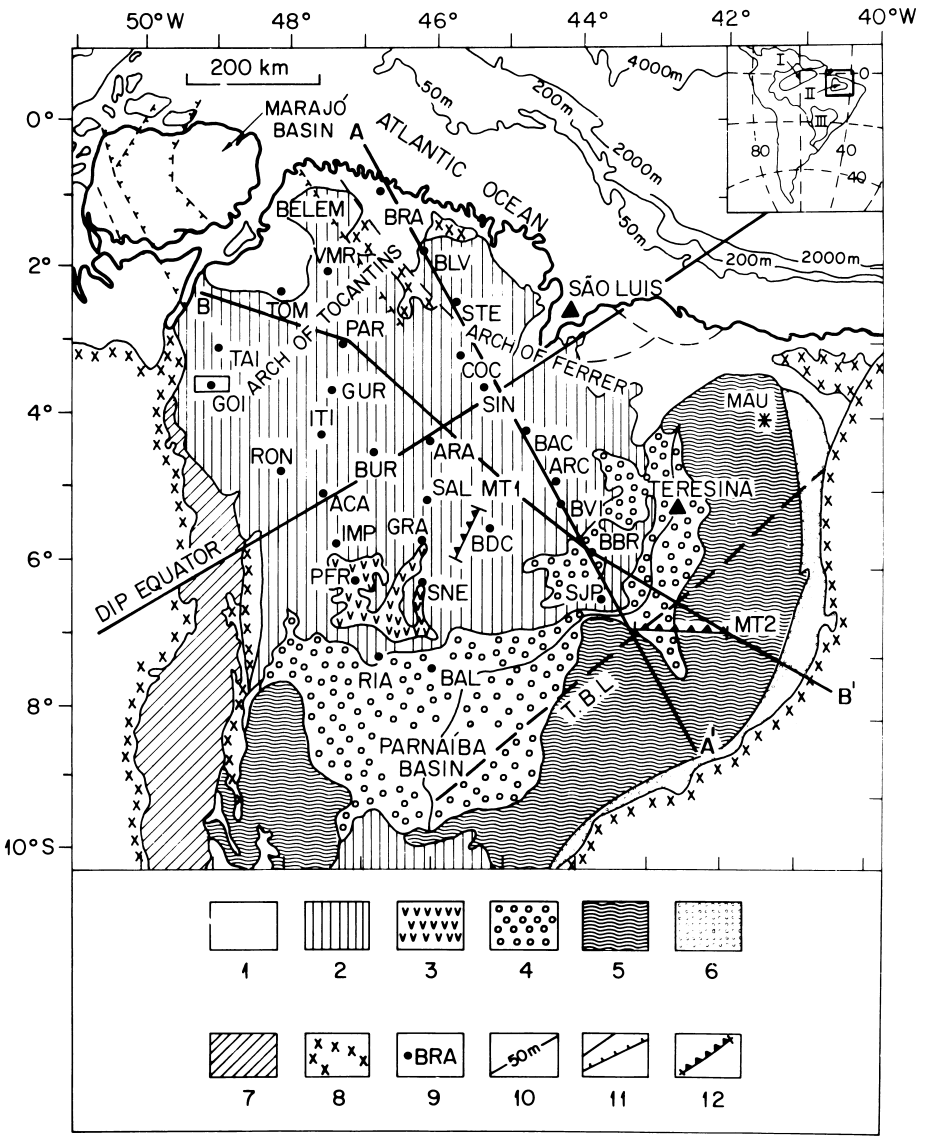

Fig. 1. Map showing the layout of the magnetometer sites (dots) in relation to the geology of the study area (modified from Mesner and Wooldridge, 1964, and DNPM, 1971). The geological classification was adopted from Góes et al. (1990, 1993), where marked legends represent: *1* = Cenozoic; *2* = Jurassic–Cretaceous; *3* = Mesozoic volcanics; *4* = Permian–Carboniferous–Triassic; *5* = Devonian; *6* = Ordovician–Silurian; *7* = Araguaia fold belt; *8* = undifferentiated Precambrian; *9* = magnetometer sites; *10* = ocean depth; *11* = trace of faults; *12* = locations of magnetotelluric profiles. Profile *A–A′* along the eastern line of magnetometers is used in the numerical modelling of the present study and *B–B′* marks the line of the geological cross-section shown in Fig. 4a. The location of the long-period MT site (*MAU*) is also marked. Station GOI was used as reference site in the computation of inter-station transfer functions. The inset shows the location of the study area and three intracratonic basins of the Brazilian shield, namely: *I* = Amazon; *II* = Parnaíba; *III* = Paraná.

The statistical-frequency analysis showed that the anomalous behavior of the MV fields at periods longer than 1 h were determined by the currents flowing in the deep Atlantic Ocean. At periods below this range, the anomalous signatures were, however, principally controlled by the current concentration in two inland conductive structures. A major one, beginning close to the center of the basin, was shown

to extend to the northeast in the southeastern part of the oval-shaped basin. A second, narrower NW–SE-trending structure was located in the area intervening between the Parnaíba and Marajó basins. These two structures were referred to as the Parnaíba Basin Conductivity Anomaly (PBCA) and the LINK anomaly, respectively. The anomalous electric character of the Parnaíba Basin, coinciding with the PBCA, was also indicated by the magnetotelluric (MT) soundings made by Oliveira and Fontes (1991) on a short MT-profile in the central part of the basin, marked in Fig. 1 as MT1. The interpretation of these MT soundings revealed an anomalously high conducting (<1 Ω m) layer in the deeper parts of the basin. This evidence of a highly conducting structure both by MV and MT techniques has important cognitive consequences (Banks et al., 1996). Firstly, the MV response measured in a 2-D spatial domain becomes a valuable way of detecting lateral boundaries of the conducting horizon, which help to trace the significance of the mapped conductive structure in the context of regional tectonics and other geophysical maps. Secondly, the high-resolution resistivity–depth distribution provided by the localized MT surveys can be used as a guide to interpret numerically the MV response in order to constrain the vertical configuration of the associated structure. The non-uniform thin-sheet model reported in Arora et al. (1997), successfully attained the first objective. The model featured the PBCA as a nearly 200 km wide NE–SW-trending block with an overall conductance (product of conductivity and thickness) of the order of 2000 S. In this paper, we report the result of a numerical modelling undertaken to define the vertical structural configuration of the PBCA as a key to its geological interpretation. A 2-D numerical modelling of the frequency-dependent MV response is carried out along the eastern line of magnetometers (profile A–A′ in Fig. 1), where the spatial response of the PBCA is best resolved and is found to be compatible with the induction in a 2-D elongated structure.

2. Magnetovariational response characteristics of the PBCA

First-hand information on the nature of the conductivity distribution within the study region is brought out by the maps of real and quadrature induction arrows. Fig. 2 gives, as a representative example, the maps of real and quadrature induction arrows for a period of 12 min. Maps for two additional periods are given in Arora et al. (1997). Parkinson's plotting convention is adopted so that the arrows point at right angles to the current concentration in high conductive zones (Gregori and Lanzerotti, 1980). The location and the extent of the

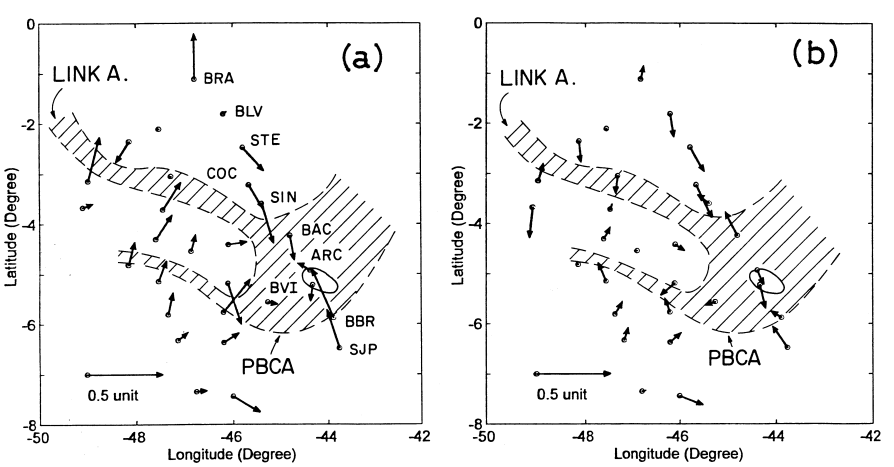

Fig. 2. Maps of (a) real and (b) quadrature induction arrows for the period of 12 min. Typical value of standard error associated with the length of arrows is 0.02 nT whereas errors in azimuth rarely exceed 10°. Coded names of the stations on the eastern profile which help to define the PBCA are also marked. The hatched zone in the background shows the area of high conductivity as mapped by the thin-sheet model (Arora et al., 1997).

high-conductance zone, as outlined by the contour of 800 S in the thin-sheet conductance model, is also superimposed. The most salient induction features were shown to be related with two anomalous current paths, the LINK anomaly in the northwest and the PBCA in the southeastern part of the array. The present paper is concerned with the PBCA, whose signatures are best seen below the period range of 1 h on profile A–A′. On the extreme south of the profile, the real induction arrows at the stations SJP and BBR point to the north-northwest, clearly indicating a current concentration to the north along the ENE–WSW path. Further up on the profile, the arrows at the STE, COC and SIN stations are directed south-southeast, limiting the position of the current concentration to within SIN (or BAC) and BBR, where oppositely directed arrows attain the maximum magnitude. The northeast-pointing arrows at SNE, GRA, define the southwestern terminal edge of the PBCA. The near-vanishing real arrow at BDC, Z tending to zero, suggests the proximity of the station to the axis of the PBCA. Station BDC is located close to the center of the basin where the thickness of the sedimentary column is largest, reinforcing the hypothesis that induced currents must be flowing in the sedimentary columns.

The accompanying quadrature arrows in Fig. 2b portray a spatial picture that corroborates the interpretation offered by the maps of real induction arrows. The parallel orientation of the real and quadrature arrows on the eastern profile A–A′ is another strong evidence that the induction response is related to a 2-D structure (Banks and Ottey, 1974). For the present discussion and interpretation, only the real parts are used, as the imaginary parts are relatively smaller and show frequency dependencies markedly different from those of the real parts. The relative strength and frequency dependence of the real and quadrature parts were used to infer the functional induction (regional or local) modes as well as the character (reactive or resistive) of the involved structures (Arora et al., 1997, 1998a).

Further information on the dimensionality/orientation and depth extent of the PBCA is gleaned from the pseudosections of the real parts of the anomalous vertical field (Z_r), constructed following the procedure outlined by Gough and Ingham (1983). The Z_r that is generated by the horizontal field of unit

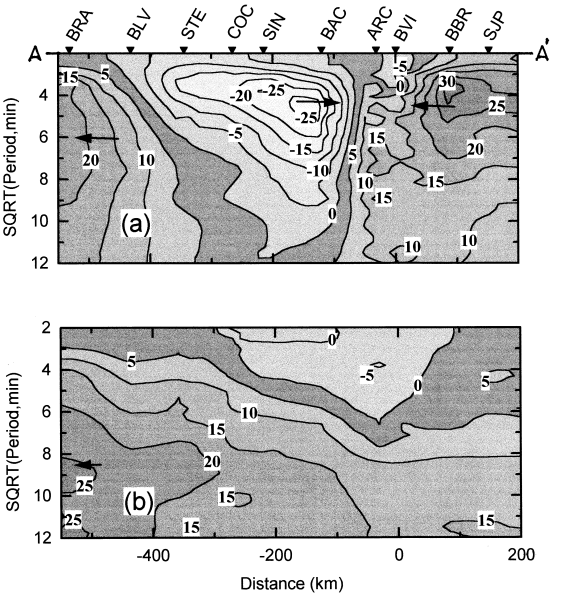

Fig. 3. Pseudosection of the real part of the anomalous vertical field ($Z_r \times 100$) associated with unit amplitude horizontal field polarized in (a) N30ºW and (b) N60ºE. Arrows point towards region of higher conductivity. The horizontal distance is marked away from station BVI in kilometers.

amplitude and specified azimuth (polarization) was estimated by performing hypothetical event analysis (Bailey et al., 1974) on the set of transfer functions. Such an evaluated Z_r field for all stations and for 13 bands of periods, for which transfer functions were computed in the earlier papers (Arora et al., 1997, 1998a), were contoured on a pseudosection for which the horizontal scale is the distance of the sites along the profile and the vertical scale is the square root of the period (T), a function of the penetration depth. Fig. 3a and 3b gives, respectively, the pseudosections of Z_r associated with the linearly polarized horizontal field in the azimuth of N30ºW and N60ºE. Consistent with the sign convention for the induction arrows, the sign of Z_r has also been reversed on the pseudosections, and, thus, a negative zone indicates the conductive source to the right, and a positive zone indicates the source to the left. At periods shorter than 1 h, a well defined couplet of positive and negative contours in Fig. 3a indicates a high-conductivity zone embedded between the locations of extreme Z_r values, i.e. between SIN and BBR. The above anomalous pattern, best de-

veloped in Fig. 3a corresponding to polarization of N30ºW, almost vanishes in the pseudosection associated with the orthogonal polarization (Fig. 3b). This polarization-sensitive anomalous behavior can most distinctly be interpreted in terms of induction in a 2-D elongated structure striking N60ºE–S60ºW. Although, the pseudosections do not provide information on the true depths of the conductive zones, the dominance of the measured response at relatively low periods can be construed to infer a relatively shallow depth of the involved structures.

Enclosed between closed contours of opposite signs are some local perturbations which become more apparent on the profile of Z_r at specific periods, shown later in Fig. 7. The small wavelength anomaly centered around stations ARC and BVI is best resolved in the period range of 10–25 min, though the pattern can be seen up to the period of 1 h. The profile of Z_r at some selected periods is a useful display of the observed induction response for comparison with the numerical response of the geoelectrical models to be developed.

In this part of Brazil, the horizontal magnetic field polarized in the northeast quadrant induces electric currents in the ocean, parallel to the coastline. The high values of Z_r seen beneath the BRA and its decaying trend away from the coastline can be attributed to the coast effect (Menvielle et al., 1982). The observation that this pattern tends to be stronger with the horizontal field polarized at right angles to the coastline (e.g. see Fig. 3b) lends support to the interpretation about their source in the oceanic region. The fields of these oceanic currents are superimposed and tend to dominate the magnetic fields associated with currents induced within the study region at periods greater than 1 h. As a consequence, at these long periods, the induction arrows at all stations point to the northeast, towards the current flowing in the deep Atlantic Ocean (Arora et al., 1998a).

3. Design of the electrical model

To find the electrical conductivity distribution model that produces an induction response similar to the observed one, a 2-D trial and error forward modelling approach was adopted. Owing to the well-known problem of non-uniqueness associated with forward modelling, the range of models tested numerically was restricted by examining the following pre-existing geological, geophysical and electrical information about the area: the attempt is to find the model which can satisfy the observed response at a wide range of periods, not just at one period, and accommodate other geophysical signatures.

4. Geological considerations

Fig. 4a shows a geological cross-section along a transect B–B′ (location marked in Fig. 1) which runs sub-parallel to profile A–A′. The section is based on six deep boreholes, widely spaced (about 100–200 km), of which only the most easterly one reached the crystalline basement. The regional geological stratification consists of a succession of three distinct sedimentary formations deposited during three megacycles and represented by the Serra Grande (Silurian), Canindé (Devonian) and Balsas (Permian–Carboniferous–Triassic) Groups (Góes et al., 1990, 1993; Góes and Feijó, 1994). Each group is separated by widespread regional discordances, which signify slow crustal oscillations of epeirogenetic origin in the tectono-evolution of the Parnaíba Basin (Cunha, 1986). The Serra Grande and Canindé Groups of rocks deposited during cycles of marine transgression and regression are exposed only along the eastern and southeastern parts of the oval-shaped basin. Near the central parts, they together account for 2700 m of the total thickness of 3400 m (Mesner and Wooldridge, 1964; Bigarella, 1973). A large northwestern part of the basin is occupied by the continental sedimentary rocks of the Balsas Group; capped by flood (volcanic) basalts of Early Jurassic and Early Cretaceous age, their total thickness rarely exceeds 800 m.

In disregard to the near-symmetric disposition of the sedimentary sublayers extending over the full range of the basin, the observed response pattern suggests a structural/conductivity complexity confined only to the central part of the basin, located between stations COC and BBR (Fig. 3). Furthermore, our test calculations have shown that when either the Serra Grande or the Canindé Group was assigned any arbitrary resistivity value over the full

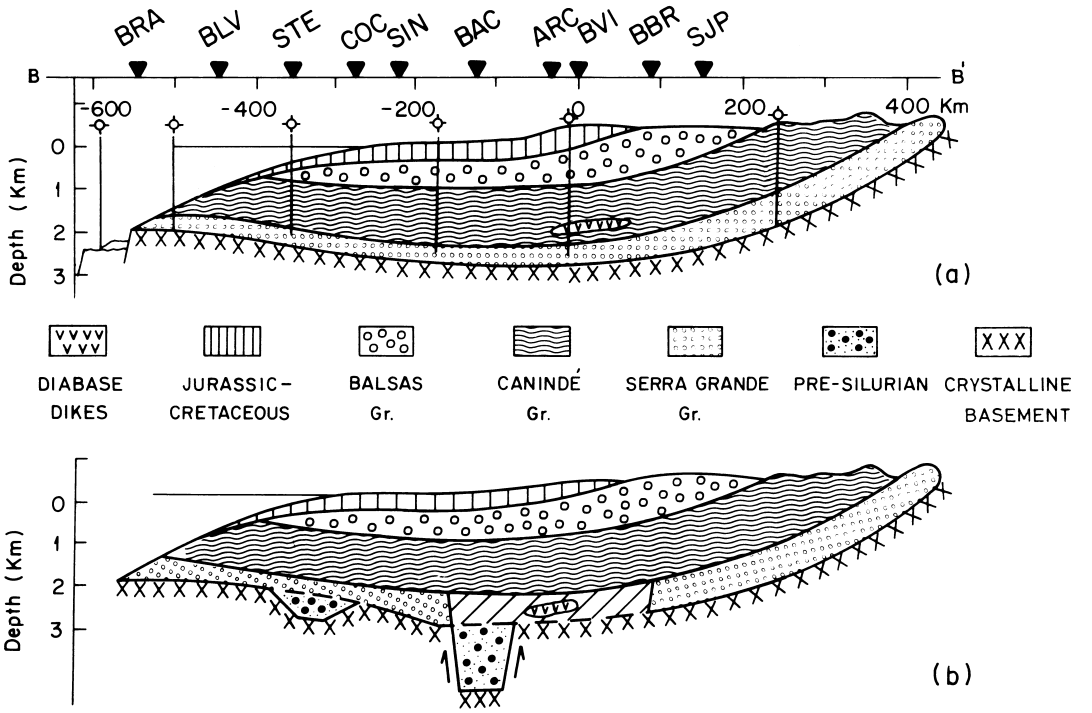

Fig. 4. (a) Borehole constrained geological cross-section along profile B–B′; location marked in Fig. 1 (adapted from Caputo and Lima, 1984). The locations of boreholes are marked by vertical lines on the section. (b) Proposed geological cross-section based on the deduced electrical conductivity distribution model along profile A–A′.

length of the basin, the resulting response held no resemblance to the observed one.

5. Geophysical considerations

Aeromagnetic data are the only high-density information available for most of the Parnaíba Basin, although as yet no quantitative interpretation has been reported. The qualitative interpretation by Nunes (1993), however, suggests a complex basement configuration, including the presence of graben structures aligned with the PBCA.

The gravity data from some 15,000 points have recently been synthesized to generate a Bouguer gravity map for the Parnaíba Basin and contiguous regions (Sousa, 1993, 1995). Except for the northern region bordering the coastal areas, the station distribution is very scarce. While the major gravity trends are determined by the tectonic elements bounding the Parnaíba Basin, the region of the basin itself is characterized by negative gravity anomalies of the order of −40 to −60 mGal. However, certain degree of structural complexity, particularly near the center, is indicated by localized gravity highs included in the regional gravity low. The presence of the gravity high coincident with the central part of the basin and enclosed in an annular low was earlier noted by Ussami et al. (1993) on the isostatic residual gravity map of the entire Brazil. However, the new Bouguer anomaly map prepared by Sousa (1993) using an updated data bank, suggests that a series of relative gravity highs flanked by gravity lows tend to extend NE–SW in the region of the Transbrasiliano Lineament. Backstripping the gravity effects of the low-density sediments, Sousa (1995) attributed the residual positive gravity anomaly over the central part of the basin to a high-density material at mid-crustal depths. Intrusion of mantle-derived material into the middle crust in response to the deep-seated extensional force have also been invoked to explain the NE–SW-trending gravity high, flanked on either side by gravity lows, in the adjoining Amazon and Paraná basins (Nunn and Aires, 1988; Molina et al., 1988; Ussami et al., 1993).

6. Resistivity assignment

For the resistivities of the various formations of the basin and the deeper layered structure, we relied on the information provided by the magnetotelluric (MT) soundings within the Parnaíba Basin or other contemporary Paleozoic basins. Extensive MT surveys by Stanley et al. (1985) in the adjacent Paraná Basin have shown that the continental Paleozoic sequence is characterized by a resistivity of 3–12 Ω m (with a central value of 7 Ω m). In the Parnaíba Basin, broad-band MT data are available at two small profiles close to the central part and on the SE margin of the basin, respectively, MT1 and MT2 in Fig. 1. MT1 is a 70 km long profile with eight soundings in the interval from 2 ms to 1000 s (Oliveira and Fontes, 1991), whereas MT2 is a somewhat longer (130 km) profile with 19 soundings in the same period interval (Sousa and Oliveira, 1995; Lima et al., 1996). At both surveys the five electromagnetic components were measured by a real-time MT system (MT-1, EMI Inc.). The MT2 profile includes scalar AMT data and Transient Electromagnetic (TEM) measurements, which were used to indicate constraints in static shift corrections and to improve the shallow-depth resolution.

The MT soundings undertaken on profile MT1 suggest the presence of a highly conductive (less than 1 Ω m) layer in the deeper part of the basin. Fig. 5a shows a MT curve, typical of those observed along that profile. The 1-D inversion of the sounding curve presents a 3-D layer structure (Fig. 5a, lower panel) for the sedimentary column above the basement. A highly conducting layer (0.1 Ω m) with an approximate thickness of 1000 m is the most dominant feature of the sedimentary section. On the other hand, the MT measurements undertaken on profile MT2 indicated a relatively less conducting (10 Ω m) layer above the sedimentary/basement interface.

The net conductance of the order of 9000 S estimated from the MT soundings at the central part of the basin is at much variance with the thin-sheet results, which estimated the conductance of the anomalous PBCA to be about 2000 S. However, as there is no additional information on the geoelectrical characteristics of the surficial sediments at the

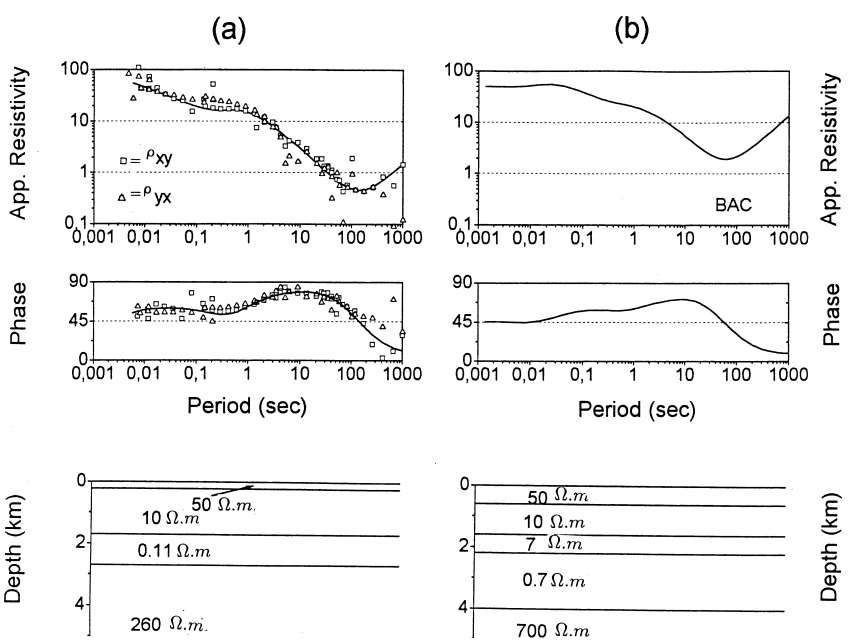

Fig. 5. (a) The observed (squares and triangles) and interpreted (continuous curve) magnetotelluric sounding at a site on the MT1 profile (see Fig. 1 for location); the lower panel gives the inverted 1-D electrical section of the above MT sounding. (b) The forward MT sounding curve corresponding to the resistivity–depth distribution beneath station BAC in the geoelectrical model of Fig. 6a. The adopted resistivity–depth section is shown in the lower panel.

region of profile MT1, no static shift correction has been applied to the MT data. Although static shift in a similar sedimentary environment of the eastern extreme of the Parnaíba Basin was estimated to be small from scalar AMT and TEM measurements (Vitorello and Padilha, 1993; Meju et al., 1997), a little bias in the estimated thickness and conductivity of the layer at the central part of the basin seems possible. In view of this, the conductivity of this anomalous block was used as a free parameter in the 2-D modelling exercise discussed below. A conductivity value of 1 Ω m or little less for the layer is found to produce a MV response comparable to the observed response and yields depth-integrated conductance compatible with the thin-sheet results.

For the range of periods considered in the present modelling, the depth penetration of induced currents (skin-depth) for a continental Earth model may vary up to several hundred kilometers. Since the parameters of the anomalous structure to be deduced from a numerical modelling are sensitive to the electrical conductivity distribution down to the full range of skin-depth (Arora, 1997), background conductivity distribution deep down the normal depths of the basin was represented by a four-layered structure (see Fig. 6a). The choice of the background conductivity distribution was based on the geoelectrical model determined by the long-period MT sounding made at a station MAU (Stoerzel, 1996), some 200 km east of the array station BAC (location shown in Fig. 1).

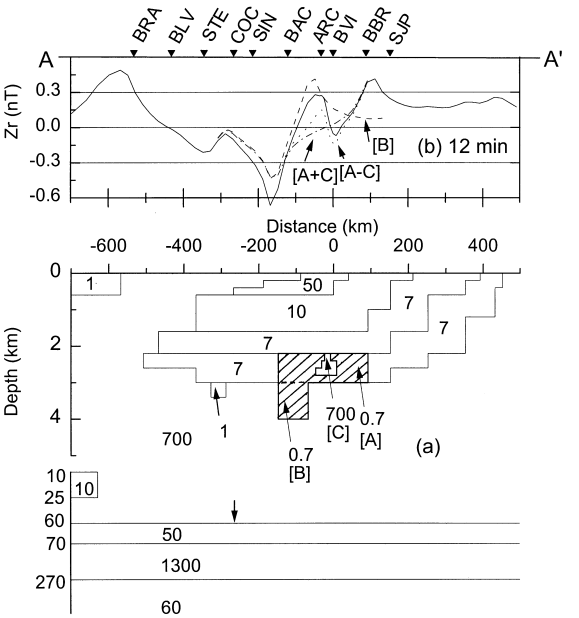

Fig. 6. (Lower panel) 2-D geoelectrical model for the Parnaíba Basin along profile A–A′. The hatched area marks the mapped inland [A, B] high-conductivity zones. Block-C denotes a resistive body intruded in Block-A. The values included in the different blocks denote electrical resistivity in Ω m. Layered structure deeper than 5 km is shown out of the vertical scale. (Upper panel) Composite induction response (solid curve) of the model at the 12-min period. Broken curve [B] shows the response when the anomalous structure zone is simulated alone by Block-B, whereas dotted [$A - C$] and dash–dotted [$A + C$] curves show the response of the Block-A with and without the embedded resistive Block-C, respectively.

7. Electrical model and its induction response

Consistent with the MT results, the source of the anomalous conductivity in the geoelectrical model was considered to be seated in the deeper parts of the basin (Fig. 6a). The lateral and vertical extent as well as the resistivity of this block (hatched area in Fig. 6a) were used as free parameters in the modelling procedure to find a match to the observation. Elsewhere, the geometry and resistivity assignment was governed by the geological cross-section and the MT soundings. Corresponding to the upper two layers in the electrical section obtained from the 1-D interpretation of the MT sounding (Fig. 5a), the exposed Jurassic–Cretaceous formations and underlying Balsas Group were assigned resistivities of 50 Ω m and 10 Ω m, respectively. Away from the central block, the Paleozoic sedimentary sequence, represented jointly by the Serra Grande and Canindé Groups, was characterized by a resistivity of 7 Ω m, in agreement with the extensive MT surveys in the adjoining Paraná Basin (Stanley et al., 1985).

The E-polarization induction response of the selected model was calculated using the numerical formulation and code developed by Cerv et al. (1987). The numerical scheme permits to simulate quite complex conductive structures by a grid of variable horizontal and vertical mesh. This facilitated approximating the overall geometry of the basin in an electrical cross-section by simple step structures. To ensure a high precision and stability in the numerical calculation of the response, care was exercised

in selecting small and nearly uniform node-spacing, particularly near the boundaries simulating the sharp conductivity contrast. In the observational domain, the horizontal node-spacing ranged from values of 4 km to 20 km. However, on either end where conductivity distribution assumes a 1-D character, the extended node-spacing was used so that the total profile length is 3–4 times the skin-depth in the layer simulating the basement. In the vertical-section, a node-spacing of 0.2 km in the shallow part was found adequate to include internal structures of the basin, whereas it varied progressively to represent the layered structure up to a depth of several hundred kilometers.

In an attempt to find the best-fitted model, the geometry and resistivities of the identified free parameters were adjusted in a trial and error process to find the match for the induction response at the 12-min period. The validity of the resulting models was tested by their ability to account for the observed frequency dependence over the range of periods for which the basic assumption of two-dimensionality was found to be valid. This requirement greatly restricted the range of models. Of the several hundred models investigated the one that reproduced the spatial as well as period dependence of the observed response is shown in Fig. 6a. The comparison of the observed and calculated response at three representative periods is shown in Fig. 7.

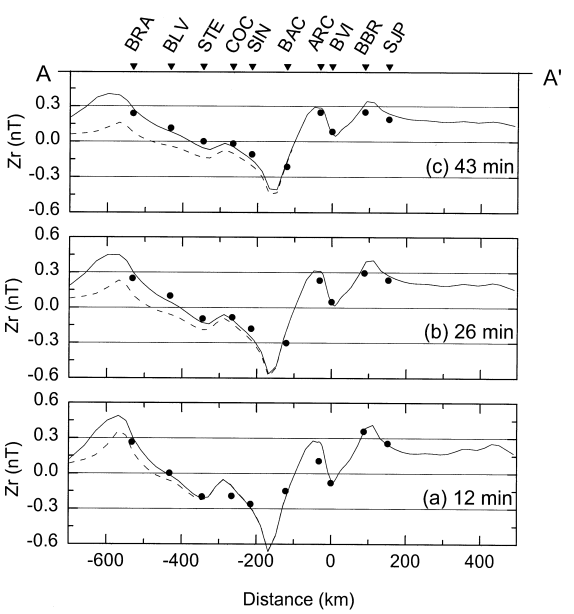

Fig. 7. Comparison of the observed (dots) and calculated responses of the geoelectrical model shown in Fig. 6 (lower panel) at periods of (a) 12 min, (b) 26 min and (c) 43 min. The broken curves show the calculated response when the conductive oceanic slab at a depth of 10 km, shown in Fig. 6, is not considered. Typical value of standard error with observed Zr is 0.02 nT.

8. Quantification of the oceanic influence

It was noted earlier that the Z_r values at the coastal station BRA are being influenced by the current concentration in the sea water. Such effects in the models were simulated by introducing a conductive sheet extending seaward from the surface position of the coastline on the NW end of the profile. Such conductive structures with well defined geometries beneath the central part of the basin in conjunction with the oceanic layer could satisfactorily reproduce the spatial characteristics of the observed response at the 12-min period. However, the model response fails to satisfy all the features of the observed response at relatively longer periods of 26 and 43 min (broken curves in Fig. 7). In particular, the degree of misfit appears to increase with increasing period on the NW flank of the profile. When an additional extended conducting slab was introduced at depth in the oceanic part of the profile, the revised (solid curve) response could account for the observed response at all periods. The Z_r values on the NW corner of the pseudosection (Fig. 3) attain the largest values at longer periods (above 1 h) rather than at the shorter periods. The inclusion of a conducting slab at depth on the oceanic side of the coastline, in addition to the conducting sea water, is consistent with this behavior of the Z_r. The effects of these oceanic conductors maximize when the incident horizontal fields are polarized at right angles to the coastline (Fig. 3b). Since the polarization which maximizes the induction in the PBCA deviates significantly from the normal to the coastline, the response of oceanic conductors included on the profile interpreted here would be only some function of the maximum coast effect. Therefore, the forward modelling would estimate electrical parameters of these conductors much lower than the actual values. This probably explains the relatively lower

conductivity value (1 S/m) for the surface oceanic layer in the model than the actual conductivity of the sea water (roughly 4 S/m).

9. Numerical validation and parameterization of the model

After suitable incorporation of the coast effect, the composite model response (solid curves in Fig. 6b and Fig. 7) is able to explain the observed response quite satisfactorily. The overall picture of the mapped conductivity model (Fig. 6a) can be viewed as an ensemble of three blocks which individually account for the distinctive features of the observed response functions (Fig. 6b). A tabular body (Block-A), roughly 240 km in width and having a thickness of the order of 800 m, is the major component of the electrical model. This wide block with a resistivity less than 1 Ω m in the central part of the basin was essential to account for the large-scale anomaly with maximum/minimum near stations COC-SIN and BBR. Consistent with the magnetic signature (Nunes, 1993), a graben-form structure (Block-B) extending into the basement is able to explain the sharp rise of the MV response observed between BAC and ARC. Another small-scale anomaly pattern between ARC and BVI could be produced by the presence of a resistive body (Block-C) embedded in the major conductive Block-A (Fig. 6a). The combined MV response of the Blocks A and B produces a minimum between SIN and BAC, much sharper than resolved by the present distribution of stations on the profile. However, any major change in the shape parameters of the blocks or their conductivity contrast with respect to the host medium alters the response curves which fails to account for either the spatial or frequency dependence of the observed response curves. Some further numerical experimentation showed that a resistivity of 1 Ω m or less was a prerequisite to produce the short-wavelength anomaly by the presence of an intrusive resistivity body. Such anomalous conducting horizon within the main body of the basin is univocally detected by the magnetotelluric surveys. In such a conductive medium, the high resistivity of the embedded intrusive was not crucial and any value higher than 200 Ω m produced the required response.

The physical validity of the model is accepted, as the adopted 1-D resistivity distribution for any site located over the graben structure (e.g. BAC) produces a magnetotelluric sounding curve with a minimum response around 100 s (Fig. 5b), similar to that observed on profile MT1. The MT measurements (profile MT2) detected a relatively less conducting (10 Ω m) layer above the sediment/basement interface and lend support to the proposed geoelectrical model that the highly anomalous layer is restricted to the central part of the basin.

In the sedimentary environment of the basin, an enhanced conductivity may generally be attributed to saline fluids in interconnected pores. However, to produce such low resistivities on the order of 0.7 Ω m or less by ionic conduction, it would require high porosities (above 12% or more; Jones and Craven, 1990). Apart from the question on the retention of large porosities in the deeper parts of the basin over such a long geological time period, it also needs to address the question why such large electrolyte-filled porosities should be restricted only to the central part, as required by the geoelectrical model.

10. Tectonic interpretation

The tectonic significance of the overall spatial conductivity distribution inferred from the magnetometer array data has already been discussed in Arora et al. (1997). The LINK anomaly appears to connect the Parnaíba Basin with the Marajó Basin and this could have served as a gateway for the transgression of the sea during some parts of the evolution of the Parnaíba Basin. The 2-D geoelectrical model developed here brings out evidence on the basement as well as the internal structure of the basin. Fig. 4b gives a proposed geological cross-section of the basin in the light of these new evidences. The formation of proposed graben structure may be related to the extensional tectonics associated with the Brasiliano orogeny (Brito Neves et al., 1984) or could have developed later in response to the crustal extension occurring as a precursors to the Jurassic–Cretaceous magmatic events (Baksi and Archibald, 1997).

During the closing phase of the tectonic–sedimentation history of the basin, two phases of

fissural tholeiitic magmatism took place. The first one in the west in Permo–Triassic time, and the second in the east during the Early Cretaceous (Brito Neves et al., 1984; Baksi and Archibald, 1997). In this tectonic scenario, the resistive body found embedded in the conductive central block of the basin may be interpreted as a diabase dike or a recrystallized magmatic body intruded during the magmatic event. A number of boreholes in the Parnaíba Basin has indeed detected the presence of such diabase intrusives (Mesner and Wooldridge, 1964). The present model, however, provides evidence on the possible dimension of these intrusives.

The positional agreement of the broad PBCA and the elongated LINK anomaly with zones of major magmatism was noted by Arora et al. (1998b). It seems that this magmatism was channelled, in part, along the pre-existing basement structures associated with the PBCA and LINK anomalies. Similar correspondence between the high conductivity zone and the magmatic activity was seen in the Pannonian Basin, where the conductivity distribution showed highest conductance near the Somlyo volcano (Ådám, 1981, 1997). This seems to indicate the causal relation between the two phenomena. The hydrous fluid released during the recrystallizing magmatic intrusion could contribute to the enhanced conductivity (Stanley et al., 1990). It also seems plausible that the enhanced electrical conductivity may be caused by the thermal effects associated with magmatic events. Laboratory measurements by Bucha (1980) have shown that when the hydrocarbon-saturated sedimentary rocks are heated above a temperature of 200ºC, films of carbon are produced by pyrolysis reactions associated with diagenesis. The presence of carbon can enhance the conductivity of the medium by several orders. The carbon-rich carbonates in the Cambro–Ordovician sequence preserved in the basement graben or thermally altered Paleozoic sediments in the central part of the basin could be the cause of the mapped enhanced conductivity zones in the Parnaíba Basin. Apart from the generation of carbon films, the pyrolysis reaction was shown to produce secondary magnetite which should produce concurrent anomalies in the magnetic data. Such an apparent relation between conductivity and magnetic anomaly was reported by Bucha (1980) in respect of the outer flysch belt around the Carpathians mountain range. The noted correlation between conductivity and magnetic anomalies in the southeastern part of the Parnaíba Basin may represent different manifestations of a single source. A quantitative interpretation of the magnetic anomaly would enable to test such a hypothesis. Similarly, the hypothesis of Duba et al. (1988), whether the light hydrocarbon lost during diagenesis of the sediments were driven off or destroyed in the region of magmatic activity, coincidently marked by high conductivity, needs to be investigated further.

11. Conclusions

By trial-and-error modelling, a geoelectrical model for the Parnaíba Basin Conductivity Anomaly (PBCA) has been obtained which explains well both spatial and period dependence of the observed response. Although the model found is by no means unique, it incorporates features imposed by magnetotelluric and other geophysical data. The proposed model locates the source region of anomalously enhanced conductivity to a sediment-filled graben structure in the basement and a conducting block with an intruded resistive body in the central part of the basin. It was also necessary to include two conducting slabs in the oceanic section to account for the period dependence of the response on the northwestern part of the inspirited profile. While the evidence on the existence of a wide conducting block confined to the central part of the basin is consistent with the magnetotelluric data, the graben structure in the basement is corroborated by the aeromagnetic data. The resistive zone embedded in a conductive medium is perhaps a manifestation of the basin-modifying tectonics arising in association with the Cretaceous magmatic activities. The spatial correspondence of the mapped conductive zones with areas of intense magmatic activity suggests that the high electrical conductivity of the medium may be due to the presence of carbon generated by thermal-controlled pyrolysis of hydrocarbon-saturated sediments. Since the pyrolysis reaction, in addition to the generation of carbon, is expected to produce secondary magnetite, a test for the proposed mechanism would be provided by the presence of

a corresponding anomaly in the aeromagnetic data. A quantitative analysis of the available aeromagnetic data would confirm this, although the noted signatures do not rule out this possibility. Complementary magnetotelluric measurements along the profile will be vital in testing and refining the model proposed here.

Acknowledgements

The field operation of the array was initiated under the FAPESP project No. 90/1024-7 and the present work is continued as a part of the CNPq funded Project No. 522342/94-9 entitled Equatorial Electrojet Related Electromagnetic Induction. Both FAPESP and CNPq are thanked for financial support. One of the authors (B.R.A.) is thankful to the Conselho Nacional de Desenvolvimento Científico e Tecnológico (CNPq) of Brazil for the award of a Senior Visiting Research Fellowship. The authors also wish to thank Naomi Ussami and an anonymous referee for critical review and constructive suggestions.

References

Ådám, A., 1981. Statistische Zusammenhange zwischen elektrischer Leitfahigkeitsverteilung und Bruchtektonik in Transdanubian (Westungarn). Acta Geod. Geophys. Mont. Hung. 16, 197–250.

Ådám, A., 1997. Interpretation of the electrical conductivity anomalies in the continental lithosphere. In: Arora, B.R., Sriniwas (Eds.), Natural Source Electromagnetic Induction in the Earth. New Age Int. (P) Ltd., New Delhi, pp. 197–250.

Arora, B.R., 1997. Geomagnetic deep sounding. In: Arora, B.R., Sriniwas (Eds.), Natural Source Electromagnetic Induction in the Earth. New Age Int. (P) Ltd., New Delhi, pp. 80–128.

Arora, B.R., Rigoti, A., Vitorello, Í., Padilha, A.L., Trivedi, N.B., Chamalaun, F.H., 1997. Electrical imaging of the intracratonic Parnaíba basin, north-northeast Brazil. J. Geomagn. Geoelectr. 49, 1631–1648.

Arora, B.R., Rigoti, A., Vitorello, Í., Padilha, A.L., Trivedi, N.B., Chamalaun, F.H., 1998a. Magnetometer array study in north-northeast Brazil: conductive image building and functional induction modes. Pure Appl. Geophys. 152, 349–376.

Arora, B.R., Vitorello, Í., Padilha, A.L., Trivedi, N.B., Rigoti, A., Chamalaun, F.H., 1998b. Geological interpretation of the Parnaíba basin magnetovariational anomaly using a 2-D sheet current inversion, Acta. Geod. Geophys. Hung. 33, 167–185.

Bailey, R.C., Edwards, R.N., Garland, G.D., Greenhouse, J.P., 1974. Electrical conductivity studies over a tectonically active area in eastern Canada. J. Geomagn. Geoelectr. 26, 125–146.

Baksi, A.K., Archibald, D.A., 1997. Mesozoic igneous activity in the Maranhão province, northern Brazil: $^{40}Ar/^{39}Ar$ evidence for separate episodes of basaltic magmatism. Earth Planet. Sci. Lett. 151, 139–153.

Banks, R.J., Ottey, P., 1974. Geomagnetic deep sounding in and around the Kenya rift valley. Geophys. J. R. Astron. Soc. 36, 321–335.

Banks, R.J., Livelybrooks, D., Jones, P., Longstaff, R., 1996. Causes of high conductivity beneath the Iapetus suture zone in Great Britain. Geophys. J. Int. 124, 433–455.

Bigarella, J.J., 1973. Geology of the Amazon and Parnaíba basins. In: Nairn, A.E.M., Stehli, F.G. (Eds.), The Ocean Basins and Margins, Vol. 1. The South Atlantic. Plenum Press, New York, pp. 25–86.

Brito Neves, B.B., Fuck, R.A., Cordani, U.G., Thomaz, A., 1984. Influence of basement structures on the evolution of the major sedimentary basins of Brazil: a case of tectonic heritage. J. Geodyn. 1, 495–510.

Bucha, V., 1980. Geomagnetism of the external flysch Czechoslovakian Carpathians and the possible causes of the anomalous geophysical manifestations. Stud. Geophys. Geod. 24, 227–251.

Caputo, M.V., Lima, E.C., 1984. Estratigrafia, idade e correlação do grupo Serra Grande–Bacia do Parnaíba, An. XXXIII Congr. Bras. de Geologia, Rio de Janeiro, pp. 740–752.

Cerv, P., Pek, J., Praus, O., 1987. Numerical modelling of geoelectrical structures in Czechoslovakia. Phys. Earth Planet. Inter. 45, 170–178.

Cunha, F.M.B., 1986. Evolução paleozóica da Bacia do Parnaíba e seu arcabouço tectônico, Unpubl. M.Sc. thesis, Univ. Federal Rio de Janeiro, Rio de Janeiro.

DNPM (Departamento Nacional da Produção Mineral), 1971. Mapa tectônico do Brasil 1:5,000,000.

Duba, A., Huenges, E., Nover, G., Will, G., 1988. Impedance of black shale from the Munsterland 1 borehole: an anomalously good conductor? Geophys. J. Int. 94, 413–419.

Góes, A.M.O., Feijó, F.J., 1994. 'Bacia do Parnaíba'. B. Geocienc. PETROBRÁS 8, 57–67.

Góes, A.M.O., Souza, J.M.P., Teixeira, L.B., 1990. Estágio exploratório e perspectivas petrolíferas da bacia do Parnaíba. B. Geocienc. PETROBRÁs 4, 55–64.

Góes, A.M.O., Travassos, W.A.S., Nunes, K.C., 1993. Projeto Parnaíba: Reavaliação da bacia e perspectivas exploratórias. Unpubl. Technical Report PETROBRÁS.

Gough, D.I., Ingham, M.R., 1983. Interpretation methods for magnetometer arrays. Rev. Geophys. Space Phys. 21, 805–827.

Gregori, G.P., Lanzerotti, L.J., 1980. Geomagnetic depth sounding by induction arrow representation: a review. Rev. Geophys. Space Phys. 18, 203–209.

Jones, A.G., Craven, J.A., 1990. The North American Central Plains conductivity anomaly and its correlation with gravity, magnetic, seismic and heat flow data in Saskatchewan, Canada. Phys. Earth Planet. Inter. 60, 169–194.

Lima, J.P.R., Oliveira, M.F.B., Fontes, S.L., Meju, M.A., 1996. Evidência do lineamento Transbrasiliano na bacia do Parnaíba

utilizando o método magnetotelúrico. An. XXXIX Congr. Bras. de Geologia, Salvador, pp. 372–375.

Meju, M.A., Fontes, S.L., Ulugergerli, E.U., Filho, A.R.S., 1997. Integration of 3-D hydrogeophysical data from Picos area in Piaui State, Northeast Brazil: Progress report. Proc. 5th Int. Congr. SBGf, Sao Paulo, SP, Vol. 2, pp. 761–765.

Menvielle, M., Rossignol, J.C., Tarits, P., 1982. The coast effect in terms of deviated electric currents: a numerical study. Phys. Earth Planet. Inter. 28, 118–128.

Mesner, J.C., Wooldridge, L.C., 1964. Maranhão Paleozoic basin and Cretaceous coastal basins, North Brazil. Bull. Am. Assoc. Pet. Geol. 48, 1475–1512.

Molina, E.C., Ussami, N., de Sá, N.C., Blitzkow, D., Miranda Filho, O.F., 1988. Deep crustal structures under the Paraná basin (Brazil) from gravity study. In: Piccirillo, E.M., Melfi, A.J. (Eds.), The Mesozoic Flood Volcanism of the Paraná Basin: Petrogenetic and Geophysical Aspects. Univ. de São Paulo, São Paulo, pp. 271–283.

Nunes, K.C., 1993. Interpretação integrada da Bacia do Parnaíba, com ênfase nos dados aeromagnéticos. An. III Congr. Int. Soc. Bras. Geofís., Rio de Janeiro 1, pp. 152–157.

Nunn, J.A., Aires, J.R., 1988. Gravity anomalies and flexure of the lithosphere at the middle Amazon basin. J. Geophys. Res. 93, 415–428.

Oliveira, M.F.B., Fontes, S.L., 1991. Magnetotelúrica na Bacia do Parnaíba: primeiros resultados. An. II Congr. Int. Soc. Bras. Geofís., Salvador 1, pp. 294–299.

Sousa, M.A., 1993. Regional gravity interpretation of Parnaíba basin (Brazil) and the L2 adjustment of a large gravity network. Unpubl. Ph.D. thesis, Univ. Newcastle upon Tyne.

Sousa, M.A., 1995. Regional gravity interpretation of Parnaíba basin, Northern Brazil. An. IV Congr. Int. Soc. Bras. Geofísica, Rio de Janeiro 1, pp. 184–187.

Sousa, M.A., Oliveira, M.F.B., 1995. Geophysical evidences of the Transbrasiliano lineament in the Parnaíba basin. An. Simp. Nac. Estudos Tectônicos, pp. 260–263.

Stanley, W.D., Saad, A.R., Ohofugi, W., 1985. Regional magnetotelluric surveys in hydrocarbon exploration, Paraná basin, Brazil. Bull. Am. Assoc. Pet. Geol. 69, 346–360.

Stanley, W.D., Mooney, W.D., Fuis, G.S., 1990. Deep crustal structure of the Cascade range and surrounding region from seismic refraction and magnetotelluric data. J. Geophys. Res. 95, 19419–19438.

Stoerzel, A., 1996. Estimation of transfer functions from magnetic variations of the equatorial electrojet — a method to determine static shifts in magnetotelluric data from equatorial latitudes. J. Geophys. Res. 101, 17917–17926.

Ussami, N., de Sá, N.C., Molina, E.C., 1993. Gravity map of Brazil, 2. Regional and residual isostatic anomalies and their correlation with major tectonic provinces. J. Geophys. Res. 98, 2199–2208.

Vitorello, Í., Padilha, A.L., 1993. Perfis de resistividade AMT: contribuição ao reconhecimento estrutural da borda sudeste da Bacia do Parnaíba. Rev. Bras. Geocienc. 23, 81–91.